A model for the evaluation of organic compounds emission from aerated liquid surfaces

Abstract

The purpose of this study is to deepen the knowledge of the various emission phenomena present in aerated tanks, widely used systems for municipal and industrial wastewater treatment.

In order to investigate the emission mechanism, a specific model was developed. The theoretical model proposes to consider three different contributions to the emission of organic compounds from aerated wastewater tanks: the convection due to the sweep air flow rate, the rising bubbles stripping and the aerosol formation and successive evaporation. To compare the modeled results, an experimental campaign was conducted with two different solutes, acetone and butanol. The sampling was carried out with a Wind Tunnel system and the outflow gas samples were analyzed with gas chromatographic technique. Moreover, this study investigates the dependence of the concentration in the gaseous phase from the speed of the air on the surface (1-5 cm/s) and from the flow of air diffused inside the liquid body (50-200 L/h). The empirical data were compared with theoretical curves. The results confirm two facts: the gas solute concentration decreases as the air velocity increases and, instead, increases with the air flow diffused through the tank.

1. Introduction

The activated sludge process is commonly used for the treatment of municipal and industrial wastewater. In this process, microorganisms oxidize organic matter to reduce the concentration of pollutants and odour releasing substances such as hydrogen sulphide and various organic compound (Hwang et al. 1995, Frechen 2004, Koh and Shaw 2017). The effective operation of the process requires the supply of dissolved oxygen to support the microbial oxidation processes that occur in the liquid phase. A common way to aerate water is via diffused air: in these systems, air is pumped through diffusers (porous ceramics, cloth or plastics) to generate small bubbles (Rosso et al., 2008). While oxygen is transferred from air to wastewater, VOCs are stripped from wastewater to air causing odour problems (Chern and Yu 1999, Gostelow, Parsons, and Stuetz 2001, Carrera-Chapela et al. 2014).

Currently, the standards of odour emission measurements on liquid area sources don't take into consideration the possible different features of this sources (Comité Européen de Normalisation, 2003), which can be quiescent or aerated.VOC emission from diffused aeration systems has already been studied. A VOC mass-transfer models, based on the American Society of Civil Engineers (ASCE) oxygen mass-transfer model, was first developed by (Matter-Müller et al., 1981) and then modified by (Roberts et al., 1984) and widely used to estimate the VOC emission rates from diffused aeration systems. A two zone VOC mass-transfer model was developed by (Chern and Yu, 1995).

This paper focuses on aeration tanks to find, and descript, the behaviour of the main parameters' influence on VOC emission. The authors developed a novel theoretical model which takes into consideration the main mass transfer mechanisms from this kind of source: the emission from the surface due to the wind convective action, the stripping from the liquid phase made by the rising bubbles, and the breaking off of the aerosol drops, due to the bubble bursting at the basin liquid

44 surface. Experiments were conducted under bubble aeration with the use of a Wind Tunnel.

45 Experimental data were compared with the values predicted by the theoretical model. In order to

46 not overlap too many variables in this preliminary study, it was decided to conduct the experimental

47 campaign with two different organic compounds, acetone and butanol, investigating the issue of

48 only one compound at a time.

1.1 Prediction of solute emission by the theoretical model

51 For the calculation of the theoretical curves a model was developed, by the authors, that includes

52 the main mechanisms of mass transfer between the aerated tank and the gaseous phase inside

53 the Wind Tunnel starting from existing models for quiescent surfaces (Invernizzi et al., 2019). The

54 basis for calculating the output concentration is the writing of the mass balance on the system, with

55 the hypothesis of stationary conditions considering the Wind Tunnel as reference volume, as

56 reported in the graphical abstract.

57 In the case of aerated basins, there are three VOC mass flow contributions coming from the liquid

58 surface of an aerated tanks:

- 59 • The convective contribution due to the sweep air flow rate inside the Wind Tunnel, which
- 60 removes VOC molecules from the liquid-air interface;
- 61 • The rising bubbles stripping contribution;
- 62 • The aerosol formation, due to the bursting of the bubbles when they reach the liquid
- 63 surface, and its successive evaporation.

64 Therefore, the steady-state mass balance of the solute in the aerated tank is:

$$Q_{out}C_{out} = Q_{in}C_{in} + K_{c,ave}(C_i - C_{bulk})A + Q_B C_B + \dot{M}_{aerosol} \qquad (1)$$

66 Where Q_{out} is the outlet airflow rate [m³/s], C_{out} and C_{in} the solute concentration in the outlet and

67 inlet airflow respectively [kg/m³], Q_{in} the inlet airflow rate through the Wind Tunnel [m³/s], $K_{c,ave}$ the

68 convective mass transfer coefficient [m/s], C_i the solute gas concentration at the gas-liquid

69 interface [kg/m³], C_{bulk} is the emitted compound concentration in the bulk of the gas phase inside

70 the hood, equal to half of the output concentration (Lucernoni et al., 2017), A the Wind Tunnel base

71 area [m²], Q_B the diffused airflow rate [m³/s], C_B the solute concentration in the bubble phase

72 [kg/m³] and $\dot{M}_{aerosol}$ is aerosol evaporation contribution [kg/s].

73 Considering a homogeneous gas phase inside the Wind Tunnel, the outlet solute concentration is:

74
$$C_{out} = \frac{K_{c,ave}C_i A + Q_B C_B + \dot{M}_{aerosol}}{\left(Q_{out} + \frac{K_{c,ave}A}{2}\right)} \qquad (2)$$

75 Considering a perfect mixing in the liquid, which is compatible with bubbling systems, the

76 convective mass transfer coefficient can be calculated as follows (Capelli et al., 2013):

77
$$K_{c,ave} = 0.664 \left(\frac{D_G^4}{L_{WT}^3 \nu}\right)^{\frac{1}{6}} u^{\frac{1}{2}} \qquad (3)$$

78 Where D_G is the diffusivity of solute in air [m²/s], L_{WT} the length of the Wind Tunnel [m], ν the

79 viscosity of air [m²/s], u the air speed inside the hood [m/s].

80 Assuming equilibrium, the Raoult's law for non-ideal liquid mixtures can be used and the solute

81 concentration at the gas-liquid interface is:

82
$$C_i = \frac{P_{sat}(T_{liq}) \cdot x \cdot \gamma \cdot MW}{R \cdot T_{liq}} \qquad (4)$$

83 Where P_{sat} is the vapour pressure [Pa], x the molar fraction in the liquid phase [-], γ the activity

84 coefficient [-], MW the molecular weight [kg/mol], R the gas constant [J/mol/K], T_{liq} the liquid

85 temperature [K].

86 A model of material transfer for the rising bubble through the aqueous solution was developed by

87 the authors.

88   The development of the theoretical model that takes into account the emission due to the diffused

89   aeration is based on the following assumptions:

90   • Constant overall mass-transfer coefficient $K_L a$

91   • Constant diffused airflow rate

92   • Rising bubbles uniformly distributed across the height of the tank

93   • Equilibrium at the interface described by Raoult's law for liquid non-ideality

94   • Homogeneous liquid-phase and constant solute liquid phase concentration

95   • Gas-phase concentration is dependent on bubble-residence time and vertical position

96   • Controlling liquid-phase resistance

97   The bubble mass balance can be written as:

98
$$\frac{dm_b}{dz} v_b = J A_b \quad (5)$$

99   Where m_B is the bubble mass [kg], v_b is the bubble velocity [m/s], J the mass flux from the liquid to

100   the bubble [kg/s/m^2], A_b the bubble surface [m^2].

101   The momentum balance on the bubble has the following expression:

102
$$\frac{d(m_b v_b)}{dz} v_b = -F_g + F_A - F_F \quad (6)$$

103   Where F_g is the weight of the bubble [N], F_A the buoyant force [N] and F_F the friction force [N].

104   Considering that:

105
$$F_A - F_g = \frac{\pi}{6} d_b^3 g (\rho_L - \rho_G) \quad (7)$$

106

107
$$F_F = \frac{\pi}{8} f d_b^2 \rho_L v_b^2 \quad (8)$$

$$f = \begin{cases} \dfrac{24}{Re} & Re < 0.3 \\ \dfrac{18.5}{Re^{0.6}} & Re \geq 0.3 \end{cases} \qquad (9)$$

108

109

110 Where d_b is the bubble diameter [m], g the gravity acceleration [m/s^2], ρ_L is the density of the liquid

111 [kg/m^3], ρ_G is the bubble density [kg/m^3], f the friction coefficient [-], and Re the Reynolds number.

112 Equation (6) can be written as:

$$\rho_G \pi \frac{d_b^3}{6} \frac{dv_b}{dz} v_b = \frac{\pi}{6} d_b^3 g(\rho_L - \rho_G) - \frac{\pi}{8} f d_b^2 \rho_L v_b^2 - J\pi d_b^2 v_b \qquad (10)$$

113

114 Then the specific mass balance on the solute has the following expression:

$$\frac{dm_c^b}{dz} v_b = J A_b \qquad (11)$$

115

116 Where m_c^b is the mass of solute inside the bubble [kg].

117 Equation 11 combined with Equation 10 allows to obtain $v_b(z)$ and m_c^b.

118 As shown in Figure 1, considering a representative first trial value for the bubble diameter, the

119 bubble velocity remains almost constant along z axis, which is the height of the tank, so we can

120 assume that the bubble immediately reaches the momentum equilibrium.
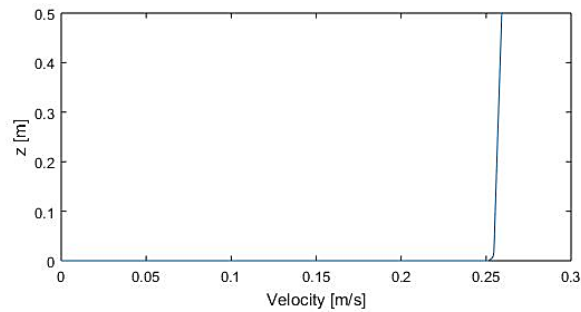
121

122 *Figure 1 Bubble velocity as function of the tank height (single column image)*

123   If the bubble is in equilibrium with the liquid phase, that is, the resultant of the forces acting on the

124   bubble is zero, the rising bubble velocity is equal to the Stokes velocity. The diameter of the bubble

125   can be calculated by the following expression:

126
$$d_b = \sqrt{18 \, \frac{v_b \mu_L}{(\rho_L - \rho_G)g}} \qquad (12)$$

127   Where μ_L is the viscosity of the liquid solution [kg/m/s].

128   For the solution of the system, the mass flux J has to be defined. The bubble is perfectly mixed

129   thanks to the internal recirculation deriving from the shear stress on the boundary with the water

130   solution during the raising; thus, the concentration inside is uniform (i.e, no resistance to the mass

131   transfer is present) (Matter-Müller, Gujer, and Giger 1981).
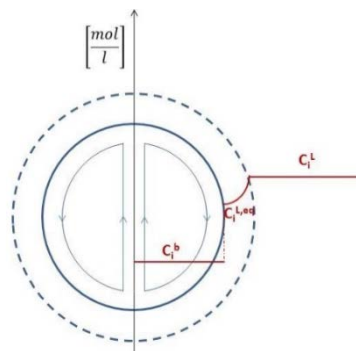
132

133   *Figure 2 Solute concentration profile at bubble-liquid interface (single column image)*

134   As sketched in Figure 2, the concentration gradient in the liquid boundary layer around the bubble

135   is given by the difference between the solute concentration in the liquid C_L and the concentration in

136   equilibrium with the solute concentration in the vapor phase inside the bubble. Thus, in mass

137   concentration, the mass flux J can be evaluated as:

138
$$J = K_{c,L} \left(C_L - \frac{C_B}{K_{eq}} \right) \qquad (13)$$

139   Where $K_{c,L}$ is the global liquid-side mass transfer coefficient [m/s], C_L the compound concentration

140   assumed constant [kg/m3] and K_{eq} a dimensionless equilibrium constant.

141   The liquid-side mass transfer coefficient $K_{c,L}$ is defined as:

142
$$K_{c,L} = \frac{Sh_B D_L}{d_b} \qquad (14)$$

143 Where Sh_B is the Sherwood number for a spherical interface, D_L the diffusivity of solute in the

144 aqueous solution [m^2/s] and d_b the bubble diameter [m].

145 In the real cases, the diffused gas is typically ambient air or cryogenic pure oxygen. Despite the

146 possible presence of VOCs in ambient air, the background concentrations can be considered

147 negligible with respect to the outflow.

148 If the entering gas bubbles contain no VOC, and the volume of the bubble remains constant, one

149 can integrate as follows:

150
$$C_B = K_{eq} C_L (1 - e^{-\frac{6K_{c,L}\tau}{d_B}}) \qquad (15)$$

151 Where τ is the residence time of the bubble in the liquid [s].

152 The quantity $K_{eq} C_L$ represents once again the concentration at the gas-liquid interface, called C_i.

153 The maximum solute concentration in the bubble is the one in equilibrium with the liquid phase.

154 Finally, it is possible to calculate the contribution deriving from aerosols entrainment. The mass of

155 compound associated with this input was calculated thanks to the expressions validated by Zhang

156 et al. (Zhang et al., 2012). It has been shown that in gas-liquid systems, the number of droplets

157 produced by the bursting of the bubble increases as the bubble size decreases. Therefore, there is

158 a critical diameter above which the bubble produces no drop by bursting onto the surface of the

159 liquid. This diameter is calculated by the following relation:

160
$$d_{cr} = \frac{10^{0.1914} \sigma_L^{0.5517}}{\rho_L^{0.483} g^{0.517} \mu_L^{0.0688}} \qquad (16)$$

161 Where σ_L is the liquid surface tension of the mixture [N/m], which can be calculated with Tamura

162 model (Poling et al., 2001).

163 The number of droplets produced by a single bubble hitting the surface of the liquid is estimated by

164 the following expression:

$$n_g = 7.9e^{-\frac{d_B}{0.338d_{cr}}} - 0.41 \qquad (17)$$

For bubble diameters between 0.1 mm and 0.9 mm the diameter of the drops is about a tenth of that of the bubble that produced them (Koch et al., 2000). If the diameter of the drops is known, it is possible to calculate their volume and from the concentration of solute in the liquid, the mass of the component entrained by each drop can be estimated.

The total mass flow linked to aerosol entrainment is given by the product between the solute mass in a single drop, the number of drops produced by each bubble and the number of bubbles:

$$\dot{M}_{aerosol} = N_{bubble}n_g m_g \qquad (18)$$

Where N_{bubble} is the number of bubbles per unit of time calculated as the ratio between the diffused airflow rate and the volume of a single bubble [1/s] and m_g the mass of solute per drop of entrained liquid [kg]. In the present study the total evaporation of all the evaporated aerosol is assumed for the theoretical model value predictions.

With the outlet concentration predicted by this mass transfer model, we can calculate the solute emission rate [kg/s]:

$$ER = C_{out}Q_{out} \qquad (19)$$

2. Materials and Methods

A series of volatile organic compounds emission tests were performed in a polypropylene tank equipped with fine-bubble diffusers made of sintered glass, with an average pore size of 60 μm. The tank has a horizontal section of 485 mm x 240 mm and a height of 0.5 m. The diffusers are

186 located at the bottom of the tank. The Emissions were measured with the use of the Wind Tunnel

187 developed by the olfactometric laboratory of Politecnico di Milano (Capelli et al., 2009). This Wind

188 Tunnel, made of PVC, has the following construction features:

189 • hood completely horizontal (central body length of 0.5 m), without any inlet or outlet flow inversion

190 curve;

191 • use of an inlet duct and a divergent (0.35 m and 0.4 m long respectively) extended in order to

192 guarantee a complete development of the fluid dynamic boundary layer;

193 • use of air flow deflecting fins inside the divergent, so that the air flow is divided into homogeneous

194 and parallel threads;

195 • constant height along the entire hood, to avoid fluid dynamic alterations.

196 The samples were collected at the outlet of the WT by means of a Nalophan® bag and a sampling

197 vacuum pump, in the same way described in (Invernizzi et al., 2019). All the samplings were

198 repeated three times, and the storage time was maintained below 6 hours. The collected samples

199 were analysed with the use of a gas chromatograph "Master GC - fast gas chromatograph" by

200 DANI INSTRUMENTS INC., with capillary column, 20m long, 0.18mm diameter and 1µm film

201 thickness. The detector used is FID (Flame Ionization Detector) whose operation is based on the

202 detection of the ions formed by the combustion of organic compounds, inside a hydrogen flame.

203 The compounds used in solution with water were acetone (Fisher scientific, purity grade >= 99%,

204 solution concentration 50 mL/L_{H2O}) and butanol (Honeywell, purity grade 99.9%, solution

205 concentration 5 mL/L_{H2O}).

206 These solutes were chosen because they comply with the following criteria:

207 • low toxicity by inhalation at the concentrations used, to minimize the risks for the operators;

208 • possibility of representing molecules and classes of molecules actually found in emissive

209 sources;

210   • detectable by gas-chromatograph.

211   We measured the steady-state concentration of the solute in the gas phase at different air

212   velocities in the Wind Tunnel for three diffused airflow rates (50 L/h, 100 L/h and 200 L/h),

213   controlled with a mass flow controller, at constant liquid temperature. The used specific diffuse air

214   flow rate (~ 1 m^3/m^2h) was chosen as representative of the lower limit of the typical real case

215   values (Eckenfelder et al., 2002). Purified compressed air was used, both for the sweep air flow

216   rate, and the diffused flow. Experimental data were compared with the results predicted by the

217   model.

218   3. Results

219   The graphs below (Figure 3 and Figure 4) show the concentration and emission rate dependence on

220   air velocity inside the Wind tunnel for acetone and butanol. Tests results at three different diffused

221   airflow rates of 50 L/h, 100 L/h and 200 L/h are shown. Experimental data are compared with

222   theoretical profiles. A comparison between resultant concentration and emission rate for the

223   different diffused airflow rates are also shown for both the VOCs under study (Figure 5 and Figure
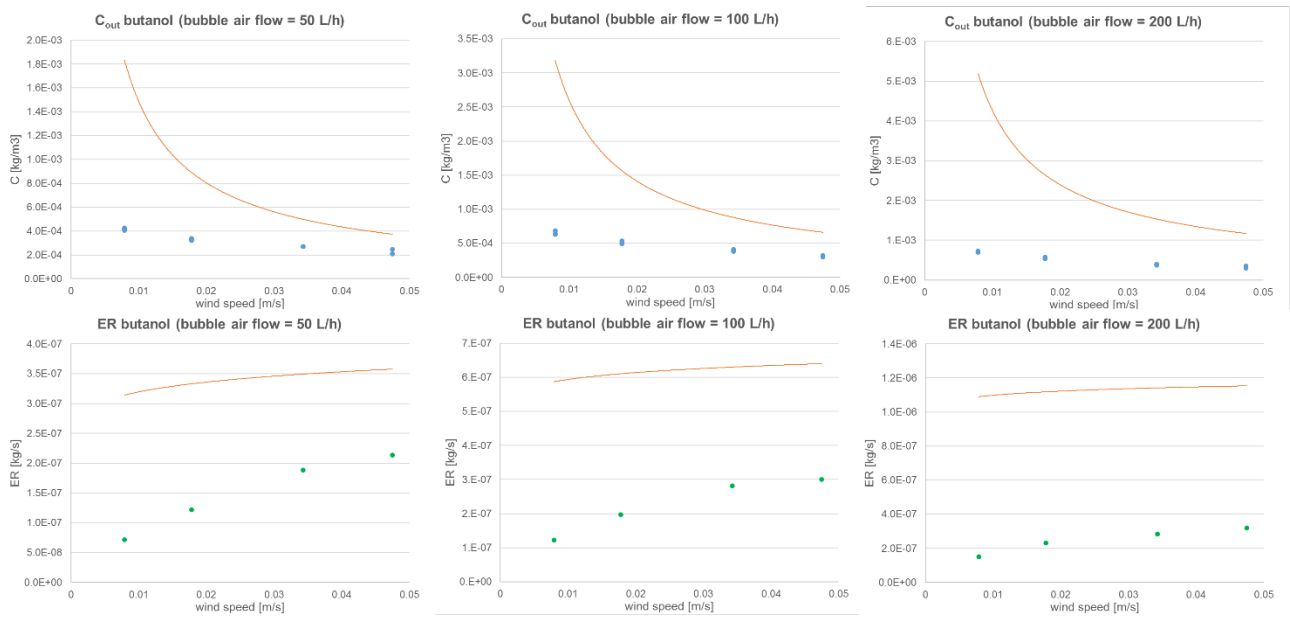
224   6).

225
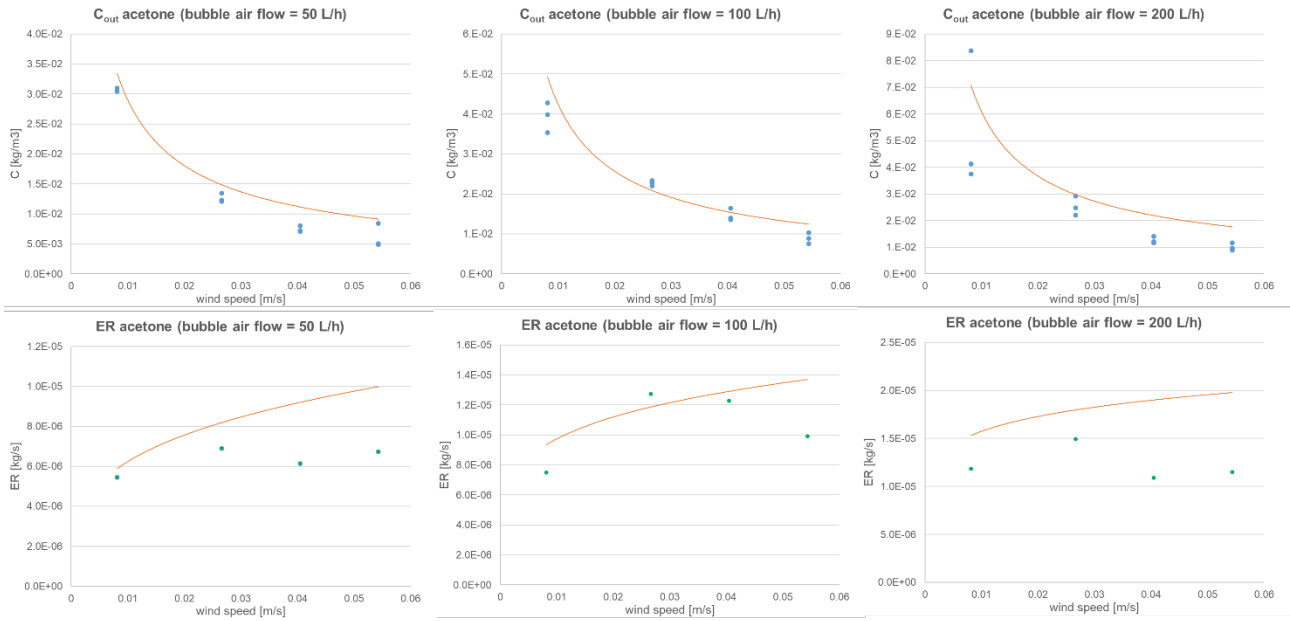
Figure 3. Outlet concentration of acetone and emission rates as function of the air speed in the Wind Tunnel for three

different diffused airflow rate. The orange solid line represents the results of the theoretical model, blue dots represent

every measured concentration, while green dots represent the average experimental emission rate. (two column page
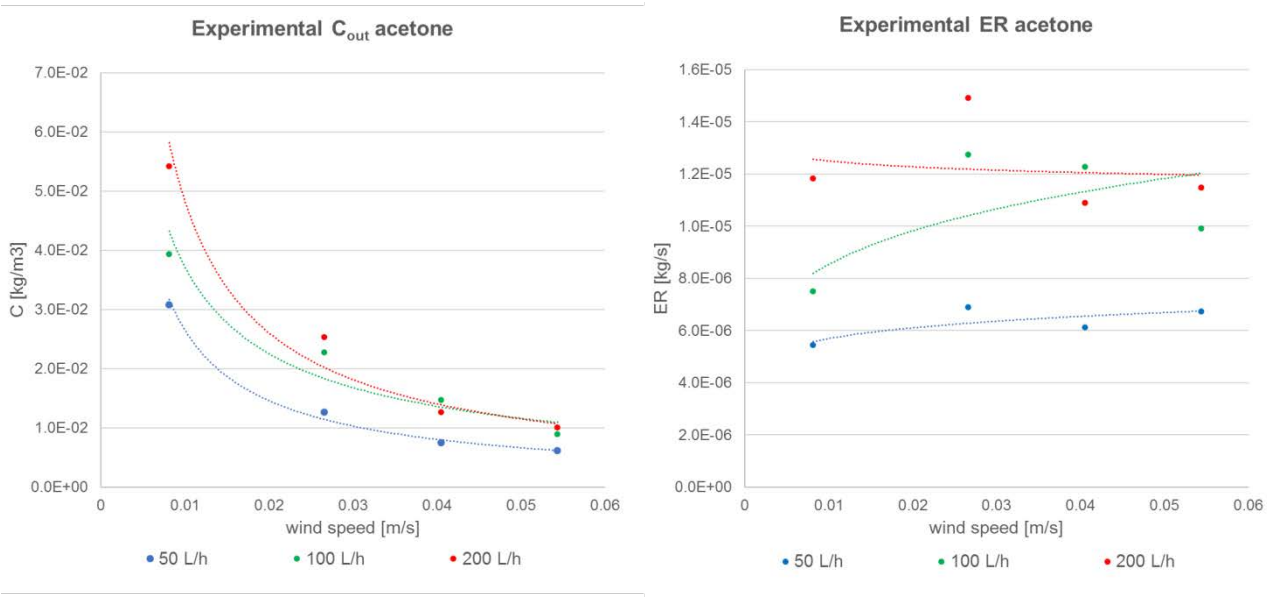
image)

230

Figure 4. Outlet concentration of butanol and emission rates as function of the air speed in the Wind Tunnel for three

different diffused airflow rate. The orange solid line represents the results of the theoretical model, blue dots represent

every measured concentration, while green dots represent the average experimental emission rate. (two column page
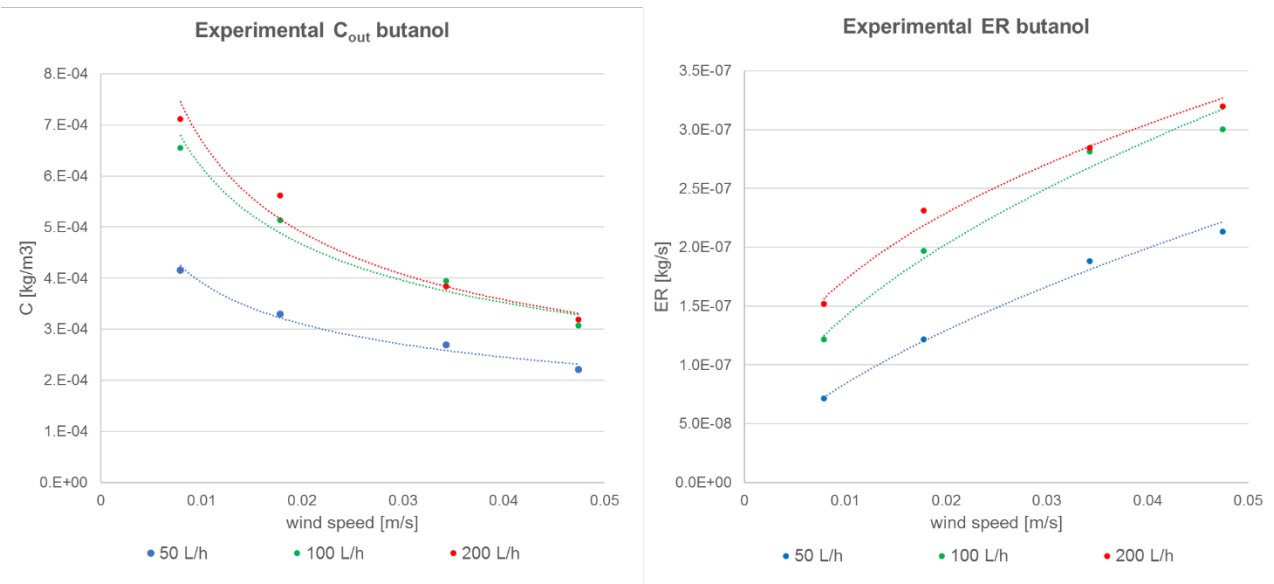
image)

235

236

Figure 5. Experimental average data for acetone solutions, aerated with different air flow rates. (two column page image)

239

240

Figure 6. Experimental average data for butanol solutions, aerated with different air flow rates. (two column page image)

Observing the acetone concentration data obtained, reported in Figure 3, it is possible to notice that the experimental curves have adherence to the theoretical lines calculated with the model.

13

In the case of n-butanol, the experimental concentration curves differ significantly from the theoretical lines (Figure 4): in every case of diffused air flow rate the theoretical model overestimate the emission by far the empirical concentrations.

The experimental concentration curves and ER were also compared for the three different flows of diffused air (50 L/h, 100 L/h and 200 L/h). It is possible to notice that there is a trend of an increasing concentration in the outflow with the growing of the diffused airflow rate. Moreover, analysing the experimental emission rates, the trend of acetone (Figure 5) appears to be flatter than the butanol one (Figure 6).

# 4. Discussion

The obtained behaviour can be linked to the physical-chemical characteristics of these compounds: acetone has a far higher volatility than butanol (boiling temperature 56 °C vs 118°C), enhancing the driving force of evaporation. In this case the assumption of total evaporation of the investigated high-volatility VOC in aerosol seems to be adequate. On the other hand, in the case of butanol solution, the model returns evaporation results far higher than the empirical ones: the lower vapour pressure of this compound make exaggerated the simplification of total evaporation of the organic compound during the time of flight of the drop.

The experimental ERs respect the assumptions reported in (Laor et al., 2014; Parker et al., 2010; Santos et al., 2012): acetone has an intermediate behaviour between the gas-phase control and the liquid-phase control, demonstrating an emission rate not dependent from the sweep air flow rate. Moreover, butanol which is a gas phase controlled compound, shows an effect of the wind speed on the evaporation mechanism.

To understand the weight of the different contributions to the emission, in Figure 7 are also plotted the trends of the various terms that contribute to the emission (i.e. volatilization, stripping and

evaporation of aerosol), for the intermediate value of diffused air flow rate (100 L/h), and the measured results. The mass flow rate linked to the rising bubbles and the one due to the entrainment of the aerosols are obviously constant, while the contribution of surface volatilization increases with increasing wind speed.
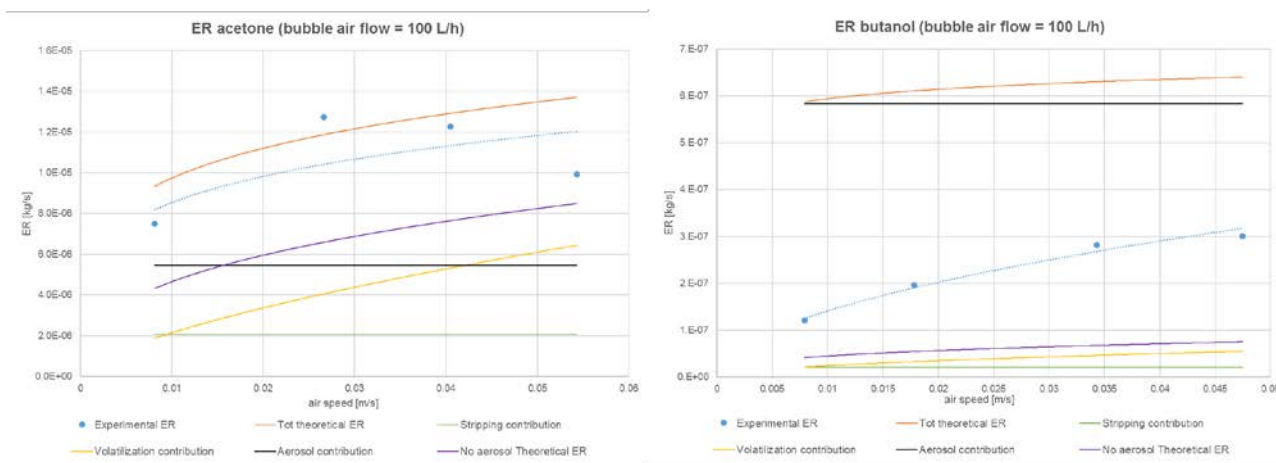
Figure 7. Comparison between different contributions to ER and the experimental ones (two column page image).

It is interesting to note that, for butanol, the term linked to the total aerosol evaporation weighs one order of magnitude more than the other contributions, while in the case of acetone has the same order of magnitude of the other terms.

As already disclosed, examining the graphs it is possible to notice that the theoretical model for the three emission contributions is adequate for the acetone trail, while overestimate the emission for the butanol trial. This difference in behaviour could be related to the difference in volatility of the two compounds. During the life time of the drop of aerosol, more volatile compounds are able to completely evaporate during the rise time, and following descent, of the drop. Furthermore, for compounds with lower vapour pressure, what appears from the comparison of the analytical results with those of the theoretical model, is that the life time of the aerosol drop is not sufficient for the complete evaporation of the compound in solution. This conclusion is also corroborated by the fact that, for the VOC at low vapour tension investigated (butanol), the most important emission contribution, estimated with the presented theoretical model, is the aerosol one (black line). At the same time, the analytical results obtained in the test with butanol (blue dots) carried in Figure 7,

288 show much higher flows than those calculated by completely neglecting the contribution of aerosol

289 (violet line).

290 From this it can be hypothesized that the evaporation of the aerosol drops have an essential

291 contribution to the global emission, but its weight is dependent on the vapour tension of the

292 compound under investigation. Considering that the emission is enhanced with aeration, not only

293 by aerosol contribution, but also by the stripping term, the increase in the emission rate linked to

294 the air through the diffusers is significant:neglecting this contributions, the total ER is significantly

295 underestimated.

296 Given that the current technical standards consider, as a limit of an active source, the specific

297 diffused air flow rate of 30 m^3/m^2h (Verein Deutscher Ingenieure, 2011) or even 50 m^3/m^2h (CEN,

298 2003), the results of this preliminary study, where the flow rates were far below these limits (~ 1

299 m^3/m^2h) advise the institutions to support investigations in the field of area source emissions.

300

5. Conclusions

301

302 The exposed work has focused on the analysis of the emission of volatile organic compound from

303 aerated tanks, such as activated sludge basin in wastewater treatment plants. The emission

304 dependence on different operating parameters was investigated for two single organic compounds

305 in water solution, and the experimental data were compared with the predicted results from a new

306 theoretical model including the main material transfer mechanisms.

307 The theoretical model developed considers that the component in solution is transferred into the

308 gas phase through three emission mechanisms: volatilization, linked to the horizontal flow of air

309 through the hood, stripping, proportional to the flow rate of diffused air, and total aerosol

310 entrainment by rising bubbles. This last term demonstrates to be not negligible but not trivial to be

estimated with precision. Experimental tests confirm that the concentration of the investigated solutes in the gaseous phase decreases as the speed of the air inside the Wind Tunnel increases, while the emission rate influence on wind speed is not the only parameter controlling the evaporation process, above all in the case of high volatile analysed VOC (acetone).

Furthermore, the theoretical model proposed here and experimental tests conducted, agree to provide for an increase in the emission with the increase of diffused airflow rate.

This work proposes a contribution to enhance the knowledge of the odorant sampling from active area source. A further proceeding of the present study can be an investigation with complex mixtures instead single VOC water solutions or a detailed analysis of the transport phenomena for the drop after the separation from the liquid surface.

ACKNOWLEDGEMENTS

References

Capelli, L., Sironi, S., del Rosso, R., 2013. Odor sampling: Techniques and strategies for the estimation of odor emission rates from different source types. Sensors (Switzerland) 13, 938–955. https://doi.org/10.3390/s130100938

Capelli, L., Sironi, S., Del Rosso, R., Céntola, P., 2009. Design and validation of a wind tunnel system for odour sampling on liquid area sources. Water Sci. Technol. 59, 1611–1620. https://doi.org/10.2166/wst.2009.123

332 Carrera-Chapela, F., Donoso-Bravo, A., Souto, J.A., Ruiz-Filippi, G., 2014. Modeling the Odor

333   Generation in WWTP: An Integrated Approach Review. Water, Air, Soil Pollut. 225, 1932.

334   https://doi.org/10.1007/s11270-014-1932-y

335 CEN, 2003. EN13725: 2003, Air quality—Determination of odor concentration by dynamic

336   olfactometry.

337 Chern, J.-M., Yu, C.-F., 1995. Volatile Organic Carbon Emission Rate from Diffused Aeration

338   Systems. 1. Mass Transfer Modeling. Ind. Eng. Chem. Res. 34, 2634–2643.

339 Chern, J.M., Yu, C.F., 1999. Volatile organic compound emission from diffused aeration systems:

340   Experiment and modeling. Ind. Eng. Chem. Res. 38, 2156–2159.

341 Comité Européen de Normalisation, 2003. EN 13725: 2003. Air quality—Determination of odor

342   concentration by dynamic olfactometry.

343 Eckenfelder, W.W., Malina, J.F., Paterson, J.W., 2002. Aeration principles and practice. CRC Pres.

344 Frechen, F.-B., 2004. Odour emission inventory of German wastewater treatment plants--odour

345   flow rates and odour emission capacity. Water Sci. Technol. 50, 139–146.

346 Gostelow, P., Parsons, S. a, Stuetz, R.M., 2001. Review Paper Odour Measurements for Sewage

347   Treatment. Wat. Res. Vol. 35, 579–597.

348 Hwang, Y., Matsuo, T., Hanaki, K., Suzuki, N., 1995. Identification and quantification of sulfur and

349   nitrogen containing odorous compounds in wastewater. Water Res. 29, 711–718.

350   https://doi.org/10.1016/0043-1354(94)00145-W

351 Invernizzi, M., Bellini, A., Miola, R., Capelli, L., Busini, V., Sironi, S., 2019. Assessment of the

352   chemical-physical variables affecting the evaporation of organic compounds from aqueous

353   solutions in a sampling wind tunnel. Chemosphere 220, 353–361.

354   https://doi.org/10.1016/J.CHEMOSPHERE.2018.12.124

355 Koch, M.K., Voßnacke, A., Starflinger, J., Schütz, W., Unger, H., 2000. Radionuclide re-

356   entrainment at bubbling water pool surfaces. J. Aerosol Sci. 31, 1015–1028.

357   https://doi.org/10.1016/S0021-8502(00)00025-2

358   Koh, S.-H., Shaw, A.R., 2017. Gaseous Emissions from Wastewater Facilities. Water Environ.

359   Res. 89, 1268–1280. https://doi.org/10.2175/106143017X15023776270296

360   Laor, Y., Parker, D., Pagé, T., 2014. Measurement, prediction, and monitoring of odors in the

361   environment: A critical review. Rev. Chem. Eng. 30, 139–166. https://doi.org/10.1515/revce-

362   2013-0026

363   Lucernoni, F., Capelli, L., Busini, V., Sironi, S., 2017. A model to relate wind tunnel measurements

364   to open field odorant emissions from liquid area sources. Atmos. Environ. 157, 10–17.

365   https://doi.org/10.1016/j.atmosenv.2017.03.004

366   Matter-Müller, C., Gujer, W., Giger, W., 1981. Transfer of volatile substances from water to the

367   atmosphere. Water Res. 15, 1271–1279. https://doi.org/http://dx.doi.org/10.1016/0043-

368   1354(81)90104-4

369   Parker, D.B., Caraway, E.A., Rhoades, M.B., Cole, N.A., Todd, R.W., Casey, K.D., 2010. Effect of

370   Wind Tunnel Air Velocity on VOC Flux from Standard Solutions and CAFO

371   Manure/Wastewater. Trans. ASABE.

372   Poling, B.E., Prausnitz, J.M., O'connell, J.P., others, 2001. The properties of gases and liquids.

373   Mcgraw-hill New York.

374   Roberts, P. V, Munz, C., Dandliker, P., 1984. Modeling Volatile Organic Solute Removal by

375   Surface and Bubble Aeration. J. (Water Pollut. Control Fed. 56, 157–163.

376   Rosso, D., Larson, L.E., Stenstrom, M.K., 2008. Aeration of large-scale municipal wastewater

377   treatment plants: State of the art. Water Sci. Technol. 57, 973–978.

378   https://doi.org/10.2166/wst.2008.218

379   Santos, J.M., Kreim, V., Guillot, J.-M., Reis, N.C., de Sá, L.M., Horan, N.J., 2012. An experimental

380   determination of the H2S overall mass transfer coefficient from quiescent surfaces at

381   wastewater treatment plants. Atmos. Environ. 60, 18–24.

382   https://doi.org/10.1016/J.ATMOSENV.2012.06.014

383   Verein Deutscher Ingenieure, 2011. VDI 3880 - Olfactometry – Static Sampling.

384   Zhang, J., Chen, J.J.J., Zhou, N., 2012. Characteristics of jet droplet produced by bubble bursting

385   on the free liquid surface. Chem. Eng. Sci. 68, 151–156.

386   https://doi.org/10.1016/j.ces.2011.09.019

387